Real time image digitizing system for measurement of air bubbles

C. VIGNEAULT[1], B. PANNETON[1] and G.S.V. RAGHAVAN[2]

[1]Agriculture Canada Research Station, Saint-Jean-sur-Richelieu, PQ, Canada J3B 3E6; and [2]Macdonald Campus of McGill University, Agricultural Engineering Department, Ste. Anne de Bellevue, PQ, Canada H9X 1C0. *[1]Contribution Number: 335/91.09.03R. Received 17 July 1991; accepted 10 December 1991.*

Vigneault, C., Panneton, B., and Raghavan, G.S.V. 1992. **Real time image digitizing system for measurement of air bubbles.** Can. Agric. Eng. 34:151-155. Bubble size is an important parameter in the determination of its behaviour in fermentation or air stripping processes used in agriculture and food industries. A method based on digital image analysis was developed to automate the measurement of bubble size and vertical velocity in a non-intrusive manner. The bubbles having a diameter varying from 0.3 to 4.0 mm were detected and measured using a thresholded digitized image. The image system was calibrated by comparing diameters measured by the camera system to the ones deduced from gas flow rate and bubble production rate measurements for both fixed and moving capillary tube bubble generators. The differences between the results obtained using these two methods of measurement were less than 0.05 mm for each diameter measured and were not correlated to the bubble size. Furthermore, the results from the two methods of measurement were not significantly different. Vertical velocity data were compared to published data.

Le diamètre des bulles est un paramètre très important pour déterminer leur comportement dans les procédés de fermentation ou de séparation de gaz utilisés dans l'industrie agricole ou alimentaire. Une méthode utilisant un système d'analyse d'images a été développé pour automatiser la mesure du diamètre et de la vitesse verticale de bulles sans interférer avec le milieu dans lequel elles se trouvent. Des bulles de 0.3 à 4.0 mm de diamètre ont été détectées et mesurées en utilisant un ton de gris seuil sur une image digitalisée. Le système d'analyse d'images a été calibré en comparant ses résultats avec ceux déduits des données obtenues à l'aide d'un débitmètre et en mesurant le taux de production de bulles de tubes capillaires fixes et mobiles. Les différences entre les résultats provenant de ces deux méthodes de mesure ont été inférieures à 0.05 mm pour chaque diamètre de bulles mesurées et ne sont pas corrélées à la grosseur de la bulle. De plus, les résultats obtenus avec ces deux méthodes ne sont pas significativement différents. Les vitesses verticales des bulles mesurées à l'aide de la caméra ont été comparées à celle de la littérature.

INTRODUCTION

The study of a theoretical model for a pressurized CO_2 water scrubber demonstrated the importance of the air bubble diameter in the gas separation process. In a bubbling system, bubbles rise from their source and their gas composition changes due to mass transfer through the gas/water interface. The main parameters affecting mass transfer are bubble volume and velocity, which determine bubble shape, together with the relevant mass transfer coefficient.

Several experimental techniques have been used for the measurement of bubble parameters. Either two- or three-dimensional systems have been used. In general, the measurement techniques can be classified in two categories depending on the nature of the sensors contacting the bubble (Lim et al. 1990). Internal sensors such as miniature capacitance/resistance probes, optical probes and static pressure probes can be grouped in the first category. Such sensors make direct contact with the bubbles. The intrusive nature of these submersible probes is expected to alter the bubble behaviour. Moreover, the characterization of the bubble size and shape from the measurement of the perceived bubble lengths requires extensive data interpretation and calibration. The second category consists of external sensors. The X-ray, γ-ray, laser and photographic methods fall into this category. These techniques provide good visual observation, thereby improving the qualitative understanding of bubble behaviour. Unfortunately, the collection of quantitative data requires subsequent frame by frame analysis of the images. This can be time consuming and laborious unless the procedure is automated.

A desirable system should as a minimum, be able to measure characteristic lengths along two perpendicular axes. This way, both bubble shape and size can be assessed. The measurement of the bubble velocity is also useful. From the preliminary analysis of the scrubbing system, it has been established that bubbles of a diameter ranging from 0.25 to 3.5 mm are required for optimum scrubber performance. Bubbles in this range have a maximum rising velocity of about 330 $mm \cdot s^{-1}$ (Clift et al. 1978). A vision system that meets the above requirements was selected based on commercially available hardware. This paper discusses the software, calibration and overall accuracy of a digital image analysis system measuring bubble diameter and velocity.

MATERIALS AND METHODS

Hardware

The experimental set-up is illustrated in Fig. 1. A 200(l) x 200(w) x 400(h) mm aquarium was built from 5 mm glass. It was illuminated on one side by a 75 W incandescent floodlight. Two diffusers assured uniformity of light intensity across the field of view of the monochrome Solid-State CCD camera mounted on a positioner on the opposite side. The camera positioner allowed movement in the horizontal plane. The entire system including the light source, the aquarium and the camera, was covered with an opaque curtain to minimize the effect of ambient light on the image.

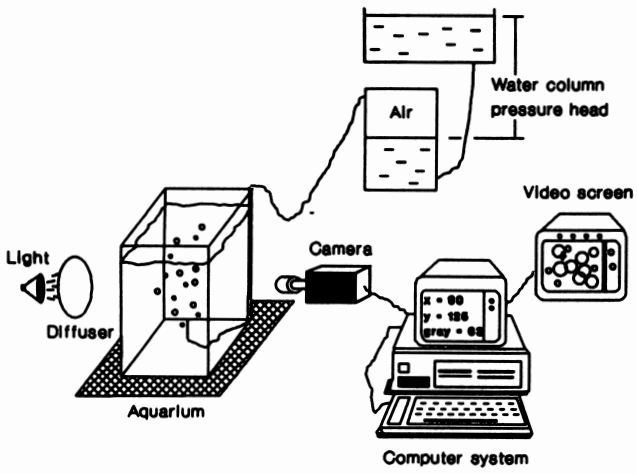

Fig. 1. Schematic of the experimental system.

The camera had a 16.9 mm scanline interlaced transfer CCD. It required a minimum scene illumination of 0.5 lm•m^{-2} at F1.4 for effective monitoring. An electronically variable shutter with nine settings ranging from 0.02 to 0.0001 s and an Automatic Gain Control circuit provided clear images over an acceptable range of light intensities. The distortion associated with the bubble motion was minimized by setting the electronic shutter at the 0.0001 s. The CCD had a resolution of 768(H) x 493(V) pixels. The video output signal had a horizontal resolution of 570 rows.

A 12.5 to 75 mm zoom lens and a close-up kit on the camera permitted a field of view of 13.5 mm across at a distance from the camera of about 200 mm. An interlaced image was formed by first scanning the odd rows after the shutter had been opened and closed. After an interval of 1/60 s, the shutter was opened and closed again and the even rows were scanned. This way, it was possible to observe, on a single interlaced image, the same moving bubble at two different positions (one on the even rows, one on the odd rows) separated by the distance it travelled during the 1/60 s interval. This feature was useful for velocity measurements.

The signal from the camera was digitized using an OCULUS-300[1] board installed in an IBM-AT compatible microcomputer. This system digitized 480 by 512 pixel images at 8 bits of resolution per pixel in real time. The board could store 4 full frames at once, and perform real time operations on images such as image subtraction.

Software

Software supplied with the digitizing board contained a set of subroutines and variables that controlled all board functions. These could be called from programs written in C language. An interpreter was also supplied which provided access to pre-programmed basic image analysis routines. However, the time required for image analysis and the flexibility of this interpreter were not suitable for this application. Dedicated software was developed to automate the measurements of bubble parameters which are described in the following sections.

Parameter measurement

Figure 2A shows a plot of grey levels as a function of pixel position for a horizontal line of pixels centred in the field of view. Since the grey level profile was fairly flat, no background subtraction was necessary. Figure 2B presents the same data when a bubble was centred on the line. When light is transmitted through a bubble immersed in water, the light rays near the centre of the bubble are transmitted with marginal attenuation and the rays hitting near the periphery of the bubble are completely reflected. This explains the characteristic shape of the signal displayed on Fig. 2B. The signal was large and bubble boundaries were well defined. A simple threshold was applied to discriminate between bubbles and background. Its level was the grey level on Fig. 2B where a maximum slope was observed, between maximum and mini-

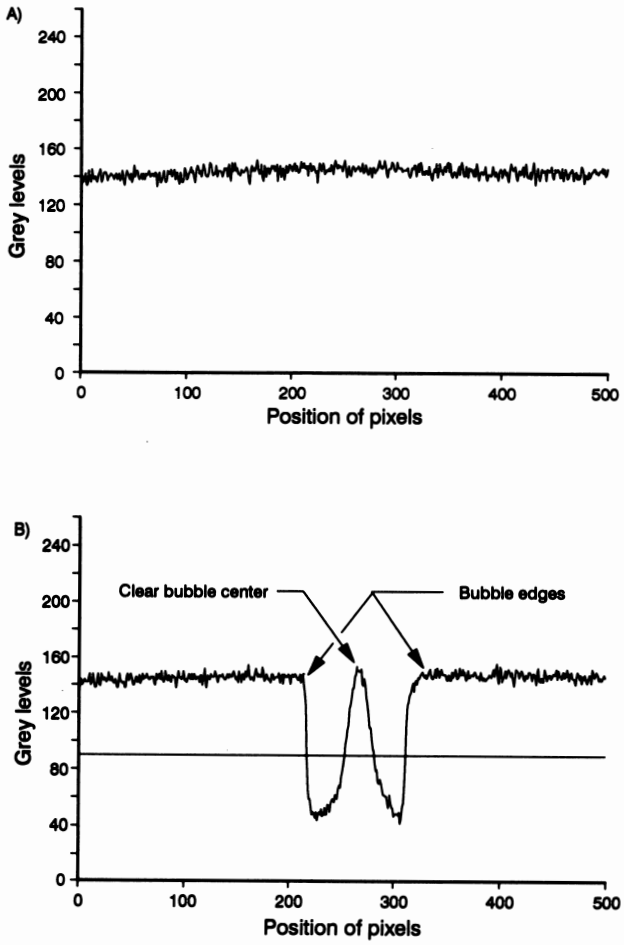

Fig. 2. Grey level along the horizontal centre line of: A) background; and B) a 2.2 mm diameter bubble centred in the field of view of the camera.

1. Mention of specific trade names does not imply endorsement of those products by Agriculture Canada or McGill University. Similary, omission of product names is not intended as discrimination against those not mentioned.

mum grey levels. A threshold level of 90 was used in all cases, resulting in good image repeatability.

To insure good repeatability, the image was focused by a technique similar to the one described by Panneton (1989). This technique maximized the slope of the grey level versus pixel position at a well defined transition perpendicular to a scan line. The slope was calculated and displayed on the computer screen. The camera was adjusted toward the object plane until the slope was maximized.

Once an image was grabbed, the system had to detect whether or not it contained a full bubble. A full bubble was defined as a set of two images of the same bubble which did not intersect the frame boundaries. As stated previously, the first image was formed on the odd numbered rows and the second image on the even rows. The image of the bubble formed on the odd rows appeared below the one from the even rows due to the 1/60 s delay.

Pixels on the even rows along a vertical line in the centre of the field of view were compared to the threshold level starting from row 2, and down. If any of these pixels had a grey level lower than the threshold, the image was discarded and the process was repeated with a new image until a pixel with a grey level lower than the threshold was found. The coordinate of this pixel was then stored to identify the image of the bubble on the even rows. The process was repeated using the odd rows but the searching started one row above the one where an image on the even rows had been found. Only when both an image on the even and an image on the odd rows were identified did the analysis proceed further.

The contour of the bubble was traced by means of a chain-coding algorithm (Reid et al. 1989). It started searching from the pixel used to identify the image on the even rows. The algorithm checked the even row pixels surrounding the current pixel in a clockwise direction, starting with the pixel next to the last unsuccessfully checked pixel. When a "good pixel" (pixel having a grey level below the clipping level) was found, the coordinate of the pixel was stored with the corresponding direction code to form a data point. The direction codes shown on Fig. 3 refer to the position of the newly found contour pixel with respect to the current pixel. The contour algorithm was repeated until it returned to the starting pixel, thereby completing the contour of the upper image of the bubble. The contour of the lower image of the same bubble was traced in the same way using the odd row data.

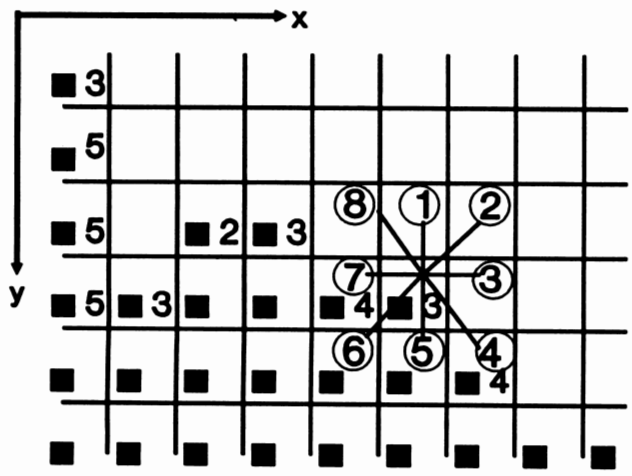

Fig. 3. Illustration of the chain-coding scheme.

The vertical diameter of the bubble was calculated from its two images. It was the difference between the maximum and the minimum Y coordinates of the pixels forming the contour of each bubble image. The horizontal diameter was calculated similarly by using the X coordinates.

The total surface, S, of a bubble on an image (projected area of the bubble) was calculated by using:

$$S = 2\,\Delta x \left\{ \left[\sum_{i=1}^{n} Y_i \right]_{dir=6,7,8} - \left[\sum_{i=1}^{n} Y_i \right]_{dir=2,3,4} \right\} \qquad (1)$$

where n = number of pixels on the contour. In the summation, Y_i was replaced by zero if the direction code of the i^{th} pixel was different from the ones given as subscripts (dir = ...).

The central axis was defined as the vertical axis which divided the surface of a bubble into two equal areas. First, the contour data were sorted in an ascending order of the X coordinates, then Eq. 1 was applied but summation stopped when X_{i-1} was different from X_i and the surface being computed was equal to or larger than half the total surface. Linear interpolation was used to locate the central axis at a point between the last two X coordinates.

The volume, V, of the bubble was calculated using the First Pappus Theorem (Ayres 1972):

$$V = 2\pi\Delta x \left\{ \left[\sum_{i=1}^{n} Y_i\,(X_i - X_c) \right]_{dir=6,7,8} - \left[\sum_{i=1}^{n} Y_i\,(X_i - X_c) \right]_{dir=2,3,4} \right\} \qquad (2)$$

where the summations follow the same rule as in Eq. 1 and X_c is the X coordinate of the centre of the bubble.

The vertical velocity of the bubble was derived by dividing the difference between the maximum Y coordinate of each image of the bubble by 1/60 s, the interval of time between the two images.

The pixel size determination was made using both the maximum and minimum useable magnification of the zoom lens. A plastic transparent ruler with 0.0508 mm divisions was used to measure the pixel dimensions along both the vertical and the horizontal axes.

Bubbles have been produced by both a stationary and a moving bubble generator. In the stationary system, two capillary tubes, 0.305 mm I.D. and 1.15 mm I.D. respectively were used for bubble generation. The capillary tubes were positioned at different angles from the horizontal to the vertical position in order to obtain different bubble sizes (Datta et al. 1950). Air was supplied to the capillary tube from an airtight reservoir maintained at constant pressure by a water column (Fig. 1), varying less than 1% over a 3 hour test period. Air pressure was measured with a U-tube manometer accurate to 9.8 Pa. A flowmeter was connected between the

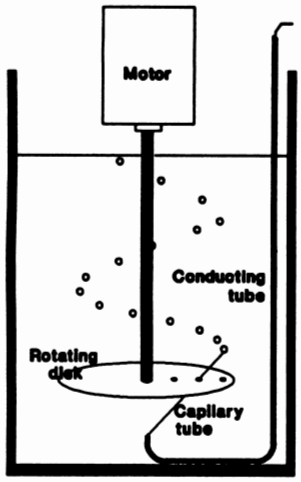

Fig. 4. Experimental set-up used to produce small bubbles.

air reservoir and the capillary tube. The complete air supply line together with the flowmeter was immersed into water to facilitate the detection of air leaks. The tip of the capillary was typically positioned at the bottom of the camera's field of view for focusing or below the field of view when bubble measurements were performed.

Smaller bubbles than the ones obtained using fixed capillary tube were produced using a rotating disk system shown on Fig. 4 using a 0.305 mm I.D. capillary tube. This system consisted of a 83 mm diameter plexiglass disk, 3.2 mm thick, mounted at the end of a 6.2 mm diameter shaft, 180 mm long. The shaft was driven by a 12 volt DC motor. Three holes, 2.8 mm diameter, were drilled on the disk at 15.7, 27.5 and 37.5 mm from the centre of the disk. The motor was mounted above the surface of the water in such a way that the disk maintained a horizontal position, 20 mm below the field of view of the camera. The capillary tube was inserted through the different holes and its end was maintained 10 mm above the disk upper surface. The tube was fixed at the bottom of the aquarium at a horizontal position coincident with the axis of the motor shaft. A DC power supply was used to control the rotational speed of the disk, which was measured with a hand-held stroboscope.

While the computer measured bubbles, the operator measured the air flow and the time required to produce 50 bubbles. Unfortunately, it was not possible to directly measure the time to produce 50 bubbles in the case of a moving tube. Thus, the rate of the bubble production was evaluated by taking the ratio of the measured linear velocity of the end of the capillary tube to the mean horizontal distance between two consecutive bubbles.

A total of 2450 bubbles was measured by the vision system. These measurements were performed on bubbles ranging in diameter from 0.34 to 4.0 mm. The results obtained from the camera and the flowmeter were used to calibrate the image analysis system.

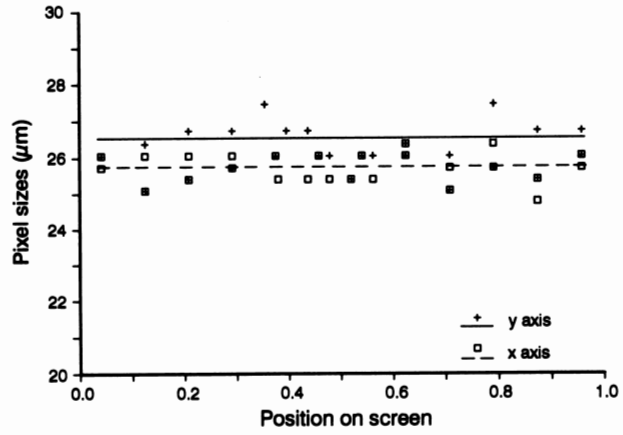

Fig. 5. Pixel size with respect to vertical and horizontal location on the screen.

RESULTS AND DISCUSSION

The results obtained from the ruler measurements allowed the determination of the pixel size at both magnification levels. The pixel size results for the maximum magnification level were plotted as a function of their position on the screen (Fig. 5). Student t-distributions were performed and confirmed that the pixel sizes are independent from their position on the screen: for X axis ($t_{1,24}$= -0.410, P = 0.68) and Y axis ($t_{1,25}$= 0.337, P = 0.74). The average pixel sizes were 0.02571 mm along the X axis and 0.02616 along the Y axis.

Bubble measurement

The volume and equivalent diameter of the bubbles were calculated using the flowmeter data and they were compared with the results from the image analysis system (Fig. 6). A linear regression was calculated that gave a slope of 0.9972 and an intercept of +0.0104. A Student t-distribution was performed on the data and confirmed that the slope ($t_{1,49}$= 0.757, P = 0.459) and intercept ($t_{1,49}$= 1.53, P = 0.133) values were not significantly different from 1.00 and 0.00 respectively. This meant that the two methods of bubble diameter

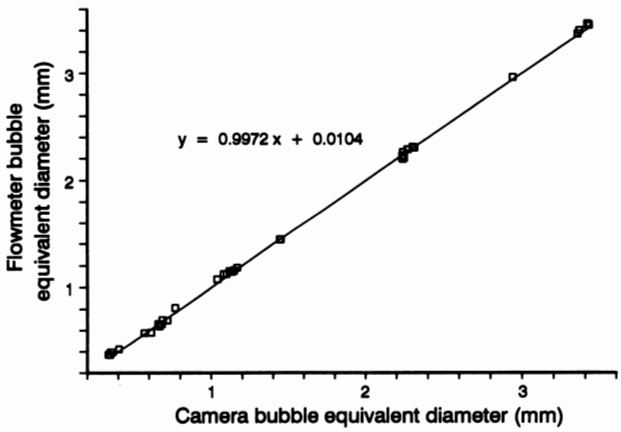

Fig. 6. Comparison between bubble diameters obtained from a flowmeter, and from the camera analysis.

measurement were not significantly different. Furthermore, the difference between the two methods of measurement was smaller than 0.05 mm or 2 pixels in size, and was not correlated to bubble size (Fig. 7).

Vertical velocity

The results obtained with the image analysis system for the vertical velocity were compared to semi-empirical values presented by Clift et al. (1978). The comparison is presented in Fig. 8. The agreement was considered good given the usual amount of scatter of such data. The velocities measured with the image analysis system were generally slightly higher than those found in the literature. The high scattering encountered for the large bubbles (D >1.3 mm) is likely due to the oscillation of the bubbles.

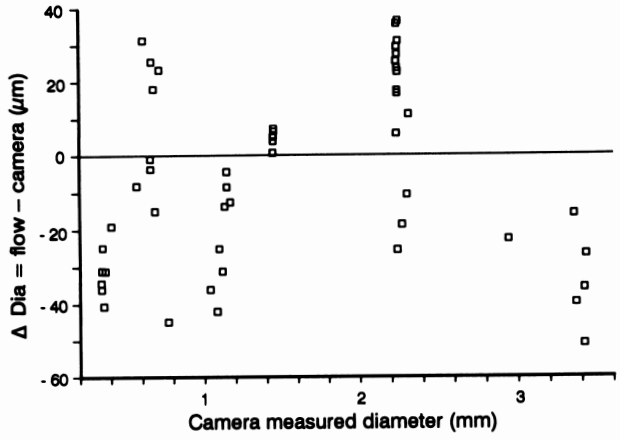

Fig. 7. Plot of differences between flowmeter and camera diameters.

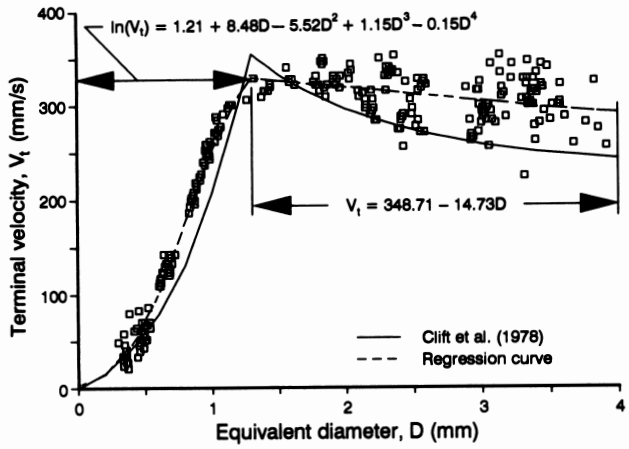

Fig. 8. Comparison between semi-empirical correlations for terminal velocity presented by Clift et al. (1978) and the results obtained using the vision system.

Regressions were computed for the terminal velocity based on collected data. These are:

$$\ln (V_t) = 1.21 + 8.48D - 5.52D^2 + 1.51D^3 - 0.15D^4 \quad (3)$$

for D < 1.3 mm; and

$$V_t = 348.71 - 14.73D \quad (4)$$

for 1.3 mm ≤ D ≤ 4.0 mm

where:

V_t = terminal velocity, and

D = equivalent bubble diameter.

CONCLUSION

A method based on digital image analysis was developed to automate the measurement of bubble parameters in a non-intrusive manner. The bubbles were identified and measured using thresholded digitized image.

Measured bubbles having a diameter varying from 0.3 to 4.0 mm were compared to flowmeter measurement. In all cases the agreement was very good. The vertical velocity measured using the image analysis system compared well with published data. Regression equations for the terminal velocity of bubbles in the range from 0 to 4 mm are presented.

REFERENCES

Ayres, F.J. 1972. *Théorie et Applications du Calcul Différentiel et Intégral*. Montréal, PQ: McGraw-Hill.

Clift, R., J.R. Grace and M.E. Weber. 1978. *Bubbles, Drops, and Particles*. New York, NY: Academic Press.

Datta, R.L., D.H. Napier and D.M. Newitt. 1950. The properties and behaviour of gas bubbles formed at a circular orifice. *Transactions of the Institution of Chemical Engineers* 28: 14-26.

Lim, K.S., P.K. Agarwal and B.K. O'Neill. 1990. Measurement and modelling of bubble parameters in a two-dimensional gas-fluidized bed using image analysis. *Powder Technology* 60(2):159-171.

Panneton, B. 1989. A system for analyzing spray samples. ASAE Paper No. 89-0017. St Joseph, MI: ASAE.

Reid, J.F. and S.W. Searcy. 1989. Machine vision: An introduction and applications. ASAE Workshop. St. Joseph, MI: ASAE.